Focal-plane wave front sensing strategies for high contrast imaging

Experimental validations on SPHERE

Jean-François Sauvage[a], Thierry Fusco[a], Cyril Petit[a], Laurent Mugnier[a], Baptiste Paul[a,b], Anne Costille[c]
[a]Office National d'Etude et de Recherches Aérospatiales, 92322 Châtillon Cedex, France
[b]Laboratoire d'Astrophysique de Marseille,
38 rue Frédéric Joliot-Curie 13388 Marseille cedex 13 France
[c] Institut de Planétologie et d'Astrophysique de Grenoble
BP 53 F-38041 GRENOBLE Cédex 9 France

ABSTRACT

Direct detection and spectral characterization of extra-solar planets is one of the most exciting areas in modern astronomy. The challenge is due to the very large contrast between the host star and the planet at very small angular separations. SPHERE (Spectro-Polarimetric High-contrast Exoplanet Research in Europe [1]) is a second-generation instrument for the ESO VLT dedicated to this scientific objective. It combines an extreme adaptive optics system [2], various coronagraphic devices and a suite of focal instruments providing imaging, integral field spectroscopy and polarimetric capabilities in the visible and near-infrared spectral ranges.

The limitation of such a high contrast imaging system is mainly driven by the presence of intensity residual in the scientific focal plane, caused by uncorrected quasi-static optical aberrations upstream of the coronagraphic mask. The measurement and compensation of these aberrations is mandatory in order to reach the level of contrast requested by exoplanet imaging.

We present in this paper the final experimental validation of the baseline method developed in the framework of SPHERE instrument for the conpensation of NCPA. The method is based on a differential measurement with phase diversity, and a compensation with an optimised modification of reference slopes.

Keywords: Adaptive optics, focal plane sensing, high contrast imaging

1. INTRODUCTION

Direct imaging and characterisation of extra-solar planets is a challenge of today's astronomy. Meanwhile, the observation of a planet orbiting a star from the ground represents a very challenging task. Such an observation requires dedicated instruments in order to separate the very large flux ratio between the planet and its host star, as well as the angular separation between the planet and the star require the use of a dedicated instrument.

The SPHERE system [1] is designed for the direct detection and characterisation of giant extra-solar planets from the ground. This instrument includes an eXtreme Adaptive Optics (AO) System (SAXO) [2] for the atmospherical turbulence compensation, providing wave-front corrected PSF to the instruments. The main limitation of such a system lies in the Non-Common Path Aberrations (NCPA), static optical aberrations introduced between the analysis path of the AO system and the scientific imaging path. These aberrations are the cause of intensity speckles in the scientific images, hence reducing the overall detectivity of the whole instrument. The measurement and compensation of such aberrations on SPHERE involves the use of a dedicated focal plane wave front sensor, based on the phase diversity technique. We present in the section 1 the implementation of phase diversity in the pseudo-closed loop, which is the baseline solution

Adaptive Optics Systems III, edited by Brent L. Ellerbroek, Enrico Marchetti, Jean-Pierre Véran, Proc. of SPIE Vol. 8447, 844715 · © 2012 SPIE · CCC code: 0277-786/12/$18 · doi: 10.1117/12.925610

for the NCPA compensation for SPHERE. We present and develop in the section 3 two solutions allowing one to mitigate these limitations.

2. PSEUDO-CLOSED LOOP: THE BASELINE FOR SPHERE

The final performance of the high contrast imaging system is mainly driven by the intensity residual in the imaging focal plane. These static residuals are due to static differential aberrations, introduced between the analysis path and the imaging path of the SPHERE eXtreme AO System SAXO, down to the coronagraph focal plane. These aberrations are commonly called "Non Common Path Aberrations", and will hereafter be designed by NCPA [4].

The measurement of these aberrations is done directly in the focal plane of the scientific detector, thanks to a focal plane wave front sensor called Phase Diversity. This focal plane wave front sensor only deals with classical imaging.

In the special case of coronagraphic imaging, where a focal mask attenuates the star signal, the main contributor to intensity residual are the NCPA introduced upstream of the coronagraphic focal mask.

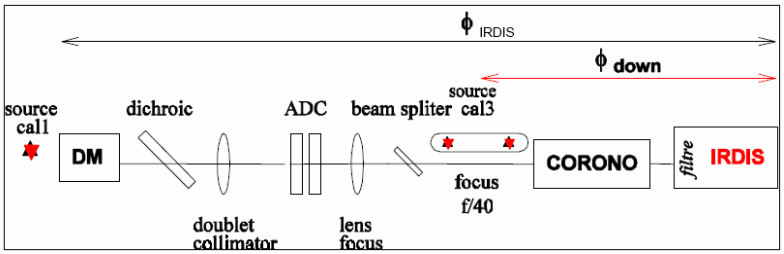

Figure 1: Optical setup for phase diversity with IRDIS: in red components that are necessary

2.1 NCPA status on SPHERE

The NCPA measurement and compensation scheme has already been validated during preliminary AIT at Meudon observatory [3]. The system available at Meudon was partially representative of the final one, as

- The Meudon system presented some high frequency optical ripples, decreasing the system performance
- The imaging was done with visible low quality camera
- No differential measurement was available => only the aberrations φ_{IRDIS} could be compensated

The SPHERE system at IPAG presents a far better optical quality; in particular no optical ripples have been constated on the bench. Moreover, the IRDIS camera offers good quality IR imaging capacity. Endly, a fibered source positioned on a motorized translation staged in the focal plane of the coronagraph allows one to calibrate the aberration downstream of the coronagraphic mask.

2.2 NCPA measurement: dedicated phase diversity algorithm

The measurement of these aberrations is done directly in the focal plane of the scientific detector, thanks to a focal plane wave front sensor called Phase Diversity. This focal plane wave front sensor only deals with classical imaging.

In the special case of coronagraphic imaging, where a focal mask attenuates the star signal, the main contributor to intensity residual are the NCPA introduced upstream of the coronagraphic focal mask. Moreover, phase diversity is not compatible with coronagraphic imaging.

2.3 NCPA optimal compensation

The compensation of NCPA is done via a modification the reference slopes of the AO loop. Closing the loop on modified reference slopes therefore allows one to pre-compensate for the NCPA. Unfortunately, at the time of this report, the compensation of aberrations has only been done with the first contributor to NCPA, which is φ_{IRDIS}. In this case, the image quality is increased on the detector itself, instead of being increased on the coronagraphic mask, which will be the final goal. The NCPA measurements performed by Phase diversity method are projected on reference slopes using calibrated matrices. The goal is to modify the reference slopes, so as to pre-compensate the NCPA with HO closed loop on modified reference slopes. The first calibrated matrix used is the influence matrix $\mathbf{F}$, gathering the pixel map response of each actuator:

$$\phi = \mathbf{F}\mathrm{u}$$

with u being the voltage vector applied to the DM, and ϕ being the corresponding phase map. The second one is the interaction matrix $\mathbf{D}$, which gathers the slopes measurement for each actuator:

$$\mathrm{s} = \mathbf{D}\mathrm{u}$$

with s the slopes measurement for each subaperture, and each direction. The slope modification Δs to apply to the reference slopes in order to compensate for the estimated phase ϕ_{NCPA} is given by the relation:

$$\Delta\mathrm{s} = -\mathbf{D}\mathbf{F}^{-1}\phi$$

with $\mathbf{F}^{-1}$ the invert of the matrix $\mathbf{F}$. This inversion is done by simple SVD routine.

2.4 Experimental results during AIT at IPAG : NCPA estimation from FP1 to IRDIS

First, the phase diversity estimation is validated with *cal1* source, which means that all optical aberrations from FP1 to IR imager IRDIS are measured. The estimation is validated on experimental data. The Figure 2 shows the acquired images, focused and defocused. The experimental conditions are the following ones :

- Date 2012 06 18
- defocus vale = 0.75 radians
- Control law = closed loop, integrator on High Order Loop
- reference slopes = center of subapertures

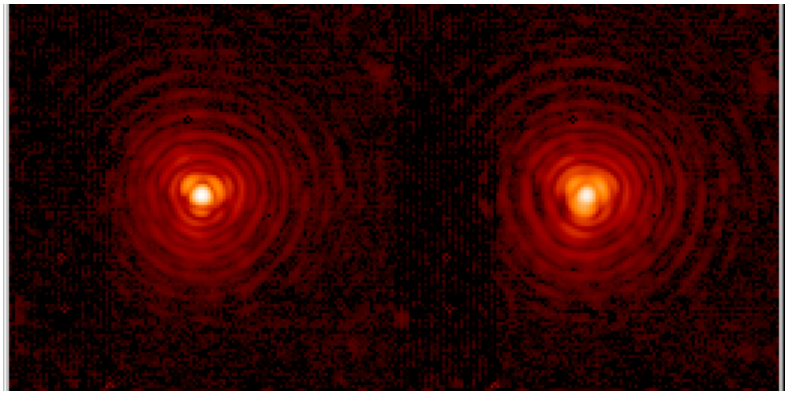

Figure 2 : Focused [left] and defocused [right] image, acquired on IRDIS imager. Defocus value is 0.75 radians RMS. No NCPA are compensated here

The Figure 3 shows the numerical images, reconstructed from Phase Diversity estimation. The result shows a good matching to the experimental data. The aberrations estimated by PD algorithm is shown on Figure 4. The aberrations are estimated on a phase map, of size 36x36 pixels.

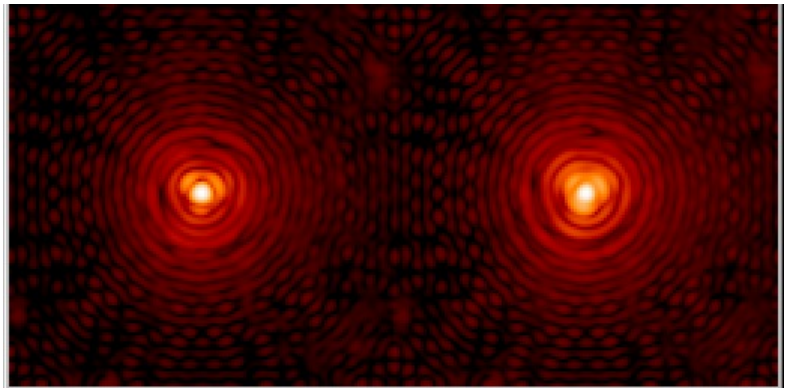

Figure 3: Numerical images, reconstructed from Phase Diversity aberrations and object measurements. A good matching with experimental data shown on is visible.

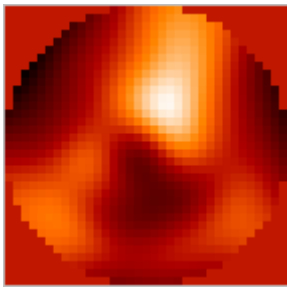

Figure 4: aberration phase map estimated by phase diversity on experimental images PV = 383nm RMS = 74nm

2.5 Experimental results during AIT at IPAG : NCPA estimation from FP3 to IRDIS

The fiber can not be positionned right into the FP3 focal plane. The two images are therefore out of focus, as shown onFigure 5. The left image is on the "focused" position, which is basically the closest to focal plane FP3. The right image corresponds to the unfocused position. Actually the calibration of FP3=>IRDIS NCPA does not include focus measurement, as the Z position of the coronagraph will benefit from a dedicated optimisation procedure.

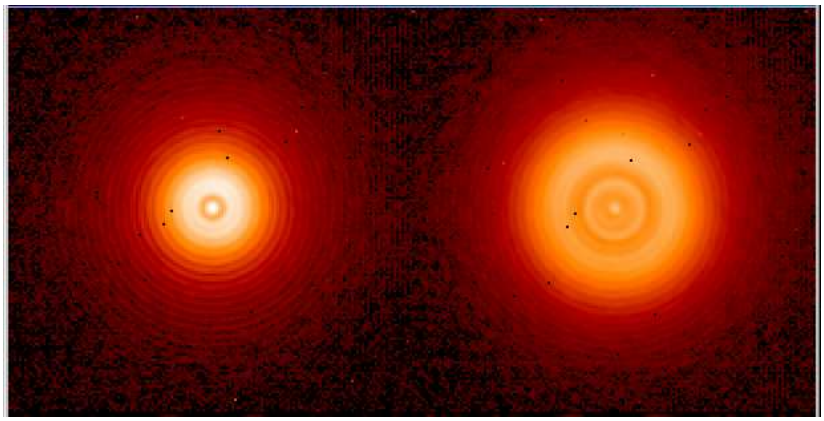

Figure 5 : images with source at FP3. Left : focused. Right : unfocused.

The first calibration to perform is to estimate

- The defocus amplitude between the two images
- The rough defocus position of "focused" image

This calibration is done by searching the minimum of a simple criterion :

$$J(a_4) = \left| i_{foc} - fh(a_4 Z_4) \right|^2$$

where i_{foc} is the focused image, a_4 and Z_4 are the Zernike coefficient and polynomial of focus, f is the flux of the image, and h is a model of the PSF with given aberration. This minimisation is done for the two focused and defocused image, and the Tableau 1 result is shown on. Left plot shows the criterion for focused image, right plot for the unfocused image. The phase of diversity is therefore constituted of a focus value a_4=2.240 radians.

Focused	**Defocused**
a_4=2.405 rad	a_4=4.645 rad

Tableau 1 : calibration of focus values in focus and out-of-focus image.

2.6 Validation of the NCPA compensation procedure

This procedure is applied iteratively, and gives the PSF shown in Figure 6. The quality enhancement is clearly visible, up to the 4th ring. The quality in the image is quantified via the Strehl Ratio (SR) estimation. It is defined as the ratio of the on-axis value of the PSF with and without aberrations. It is equivalent to a computation in the Fourier space of the ratio of integrated OTF.

$$\mathrm{SR} = \frac{\mathrm{PSF}(0)}{\mathrm{Airy}(0)} = \frac{\int \mathrm{FTO}(f)}{\int \mathrm{FTO}_{\mathrm{Airy}}(f)}$$

The computation in Fourier space allows to simply account for instrumental effects as CCD response, Object intensity map :

$$\mathrm{SR} = \frac{\mathrm{PSF}(0)}{\mathrm{Airy}(0)} = \frac{\int \mathrm{FTO}(f)}{\int \mathrm{FT}_{\mathrm{CCD}} \times \mathrm{FT}_{\mathrm{OBJET}} \times \mathrm{FTO}_{\mathrm{Airy}}(f)}$$

The Tableau 2 gives the Strehl Ratii estimated in the images, without and then with NCPA compensation, with respect to the number of iteration of the PCL procedure. A comparison is done with the Strehl Ratio computed directly from the phase diversity measurement. The very high value of 99.9% of Strehl Ratio is reached after two iterations of PCL procedure. This value includes a correction of the CCD response and the object structure. The error bar of this value has been estimated at +-1.0%.

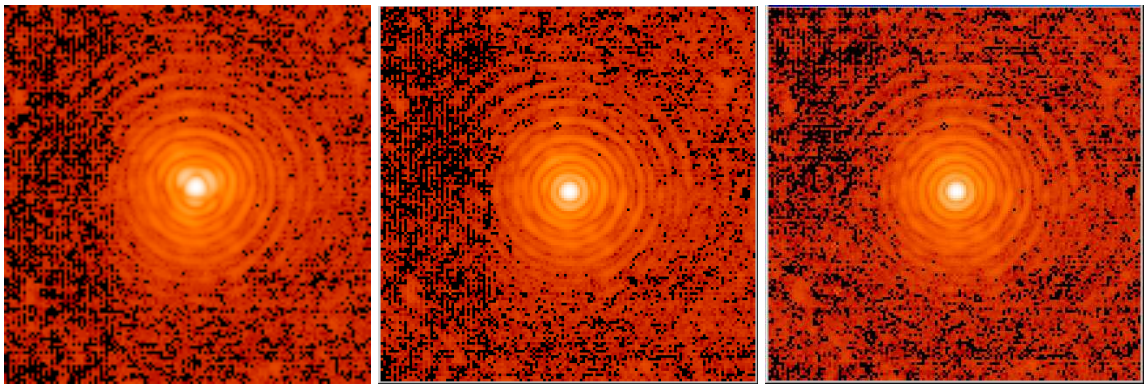

Figure 6 : Focal plane PSF. Without NCPA compensation, with 1 and 2 iterations of NCPA compensation.

	OTF + CCD + Object	**OTF + CCD**	σ_ϕ^2
Without compensation	92.0	84.2	91.5
With 1 iteration compensation	98.6	91.6	98.2
WIth 2 iterations compensation	99.9	94.0	99.6

Tableau 2: Strehl ratio estimated in the focal plane images.

2.7 Limitations of the baseline

The baseline solution proposed for SPHERE allows very high performance and fully respects the specification required in order to reach the contrast required by exoplanet imaging. However, the baseline presents some limitations. The limitations are two fold:

- The signal to noise ratio far from the optical axis of the PSF is weak. This is mainly due to the high flux ratio existing between the core of the PSF and the airy rings at the edges of the AO halo correction.
- The baseline uses a differential measurement in order to retrieve the aberrations upstream of the coronagraph. This point implies an increase of the noise on measurement (by a factor of sqrt(2) due to differential measurement). Moreover, the complexity of the system is increased, as it imposes to remove the coronagraph, and to insert a calibration fiber at the coronagraphic focal plane position, which is already extremely populated.

In order to release these two limitations, a simple solution is to use coronagraphic images instead of classical images. On the first hand, as the coronagraphic device suppresses the Airy pattern, it drastically reduces the flux ratio between the central core and the edges of corrected area, as it can be shown on Figure 7.

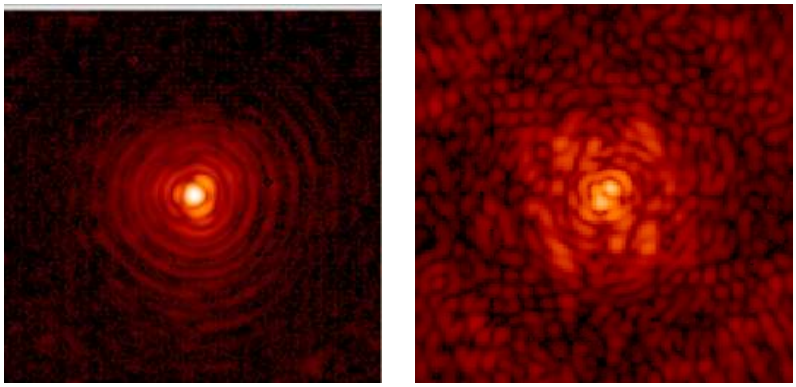

Figure 7 : classical image [left] and coronagraphic image [right] obtained with SPHERE IRDIS imager. Coronagraphic mask used is a Four Quadrant Phase mask, with Closed HO Loop, and uncorrected reference slopes.

On the other hand, using a coronagraph allows one distinguishing between aberrations present upstream and downstream the coronagraphic mask. It is known that the upstream aberrations are the main contributor to the speckle structure visible in the image.

3. IMPROVEMENT OF FOCAL PLANE SENSING

3.1 Extension of phase diversity to coronagraphic images

In order to deal with coronagraphic images, the phase diversity algorithm has to be modified. The modification required implies the use of a coronagraphic model for image formation. The model used here is the one developed in [5]. In a simplified form, it can be synthesized as:

$$J(\text{parameters}) = \sum_{\text{images}} \sum_{\text{pixels}} \left| \frac{i_{\text{data}} - i_{\text{model}}(\text{parameters})}{\sigma} \right|^2 + J(\text{parameters})$$

with a coronagraphic model of image i_{model} .

Assuming hereafter that the observed object is a point-source, a discrete model of these images is:

$$i_{\text{model}}(\text{parameters}) = f\, h_d\, h_c(\phi_{\text{upstream}}, \phi_{\text{downstream}})$$

Concerning the parameters, we distinguish between the upstream aberrations ϕ_{upstream} introduced upstream of the focal plane mask, and the downstream ones $\phi_{\text{downstream}}$.

We adopt a Maximum a posteriori (map) approach and estimate the aberrations and the flux f that are most likely given our recorded images and our prior information on the aberrations. This approach boils down to minimizing the neg-log-likelihood of the data, potentially penalized by regularization terms on ϕ_{upstream} and $\phi_{\text{downstream}}$ designed to enforce smoothness of the sought phases.

As in conventional (non-coronagraphic) phase diversity, we shall assume that we use the focal plane camera to record at least two images that differ only from a known aberration, or diversity phase ϕ_{div} , which can be introduced conveniently

upstream of the coronagraphic mask by the DM of the AO sub-system. We shall denote by i_c^f and i_c^d these focal and phase-diverse coronagraphic images.

Like in the classical phase diversity, the parameters are estimated via the iterative minimization of the given criterion.

The Figure 8 [left-bottom] shows the experimental images obtained on a coronagraphic bench at ONERA. The coronagraphic mask is a Roddier and roddier phase mask. Wavelength is 677nm. The Figure 8 [Left-top] shows the PSF computed from the parameters estimated by COFFEE. The Figure 8 [right] shows the decomposition of these parameters on the Zernike basis, troncated to 36 modes.

The COFFEE technique, used instead of the classical phase diversity, presents the following advantages :

- As the airy pattern has been suppressed, therefore the flux ratio between the central core and the airy rings far from optical axis is decreased. The dynamic of the detector therefore allows one to enhance the SNR on the high spatial frequencies.
- The image formation model for coronagraphic images naturally distinguishes between aberrations upstream and downstream of the coronagraphic mask. These parameters are then easily estimated by a criterion minimisation.

A complete characterization of the COFFEE estimator, as well as experimental results can be found in [6 (submitted)] and [7 (this conference)].

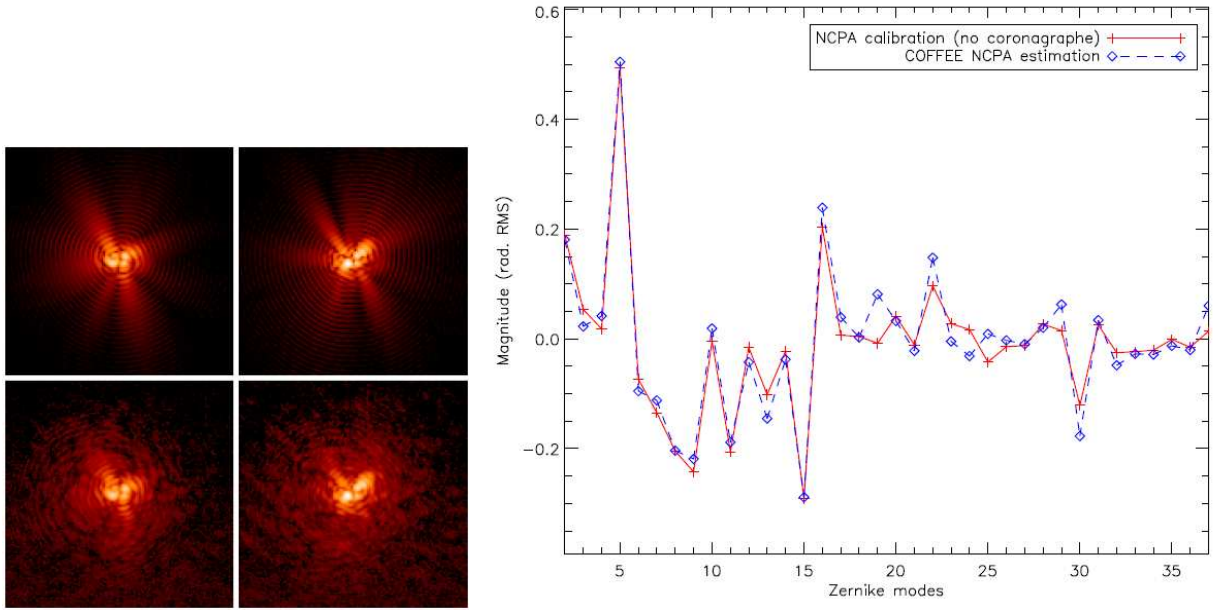

Figure 8 : COFFEE estimation of a calibrated phase map. 36 Zernike coefficients are estimated. Estimation error is 3.10^{-2} rad per mode.

3.2 Dark hole phase diversity

Both classical and coronagraphic phase diversity are based on an image formation model. For the classical phase diversity, the Fourier model is used. It assumes that phase aberrations are introduced in the pupil plane, as well as uniform pupil intensity profile. For the coronagraphic phase diversity, the model is based on a Fourier analysis. In this model, the aberrations upstream and downstream the coronagraphic mask assumed to be introduced in a pupil plane.

One of the limitation common to these two techniques relies on the relevance of the image formation model. Of course if the model does not correspond to image i_{data}, the estimation (with classical phase diversity, as well as with COFFEE), will be biased.

In order to release this limitation, we propose a simple extension of phase diversity, called "Dark hole phase diversity". This technique is still based on the same principle as the previous ones, which means the minimization of a Likelihood criterion. The criterion is modified as follows:

$$J(\text{params}) = \sum_{\text{images}} \sum_{\text{pixels}} \left| \frac{i_{\text{data}} - i_{\text{model}}(\text{params})}{\sigma[k]} \right|^2 + J(\text{params})$$

with $\sigma[k]$ being the standard deviation of the noise in pixel *k*. This parameter acts as a function that weights the pixel information. This function is usually computed from the noise model of the image (electronic noise and photon noise), but in this case we use this function to select an area of interest in the field of view.

As an example, the Figure 9 shows the phase diversity products in a classical case. This means with a uniform variance map. The central map shows a simulated aberrated PSF, 0.3 radians. This map is taken as an input i_{data}. The map on the right shows the i_{model} map, which is the PSF computed from the parameters estimated by phase diversity. The estimation is done on a pixellised phase map. The map on the left shows the criterion map, which is the value of the criterion J for each point of the field of view, which is the criterion of previous equation before summation on the pixels. The minimisation of the criterion in the classical case leads to a uniform minimisation. The residual is approximately the same for the whole field of view, the average value is 3.10^{-12}, in arbitrary units. This value is linked to the minimisation threshold

In the case of the variance map of Figure 10, an area of 8 lambda/D over 16 lambda/D is selected by using high values (10^6) outside of this area, and small values (1) inside of the area. The area is visible as grey rectangle on the Figure 10.

The following example of Figure 11 shows the same maps as Figure 9, but the minimisation is performed with the variance map of Figure 10. The criterion map therefore shows a dark hole pattern situated on the area selected by the variance map, showing an enhanced minimisation. (The display dynamic is the same for all the maps of Figure 9 and Figure 11). The criterion average value inside the dark hole region is 7.10^{-15}, while average region outside dark hole region is 3.10^{-10}.)

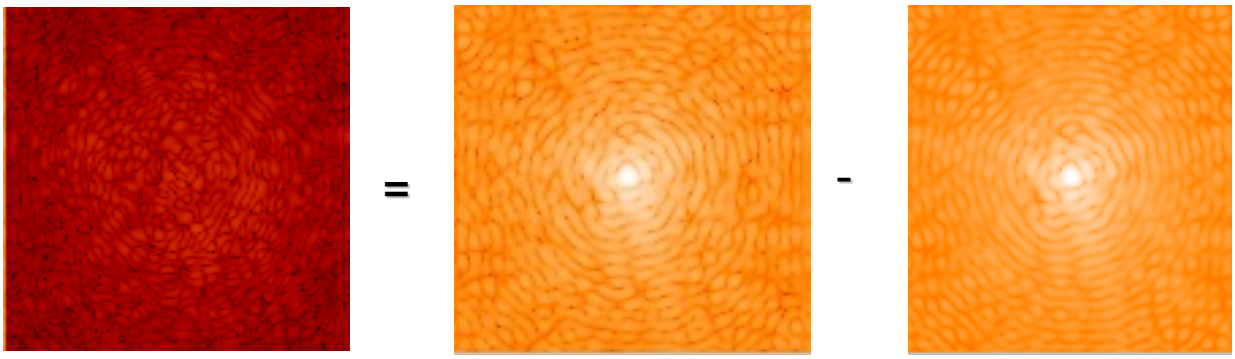

Figure 9 : [left] criterion map, which is the value of J for each pixel of the field of view, at convergence. Average value is 3.10^{-12}.
[center] i_{data} image
[right] i_{model} image at convergence.

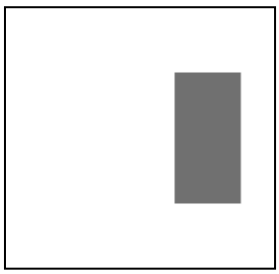

Figure 10 : weighting function $\sigma[k]$ for the whole field of view. White value is 1, gray value is 10^{-6}.

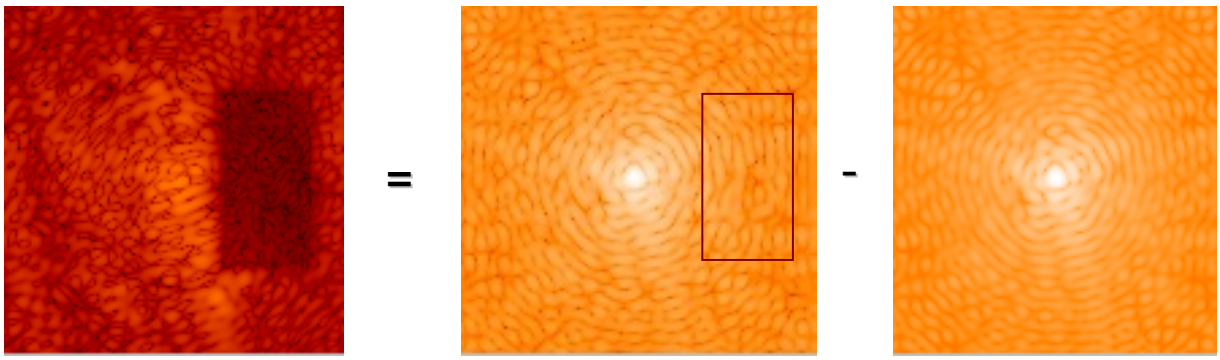

Figure 11 : Same maps as in Figure 9, but with variance map of Figure 10.
Average value inside dark hole region is 7.10^{-15},
average value outside dark hole region is 3.10^{-10}.

4. CONCLUSION

The focal plane sensing technique called phase diversity is the keypoint of the baseline procedure for SPHERE NCPA measurement and compensation. This baseline procedure has been implemented on SPHERE instrument, and allows one to reach the extreme specifications required by the high contrast imager. More than 99% Strehl Ratio have been demonstrated during SPHERE AIT.
In order to further improve the technique performance, the limitations of this technique have been developed. Possible improvements have been developed and proposed in this paper. Firstly, the coronagraphic phase diversity COFFEE deals with coronagraphic images. This allows one to increase the off axis speckle signal to noise ratio, and also estimated the upstream and the downstream aberrations in a single measurement, on the contrary to the baseline solution. On the second point, the dark hole phase diversity has been proposed, in order to adress the limitation of the image model robustness. The selection of an area in the field of view allows one to enhance the reconstruction on this area, to the detriment of the reconstruction outside of the area. In order to improve the NCPA measurement and compensation for the next generation of high contrast imagers, the future techniques will have to gather the proposed improvements, and process directly the coronagraphic images, coupled with a dark hole capacity to limit the model uncertainties.

REFERENCES

[1] J.-L. Beuzit, D. Mouillet, C. Moutou, K. Dohlen, P. Puget, T. Fusco, and A. Boccaletti, "A planet finder instrument for the VLT," in Proceedings of IAU Colloquium 200, Direct Imaging of Exoplanets: Science & Techniques, Cambridge University Press, pp. 317-323, (2005)

[2] T. Fusco, G. Rousset, J.-F. Sauvage, C. Petit, J.-L. Beuzit, K. Dohlen, D. Mouillet, J. Charton, M. Nicolle, M. Kasper, P. Baudoz, and P. Puget, "High-order adaptive optics requirements for direct detection of extrasolar planets: Application to the SPHERE instrument, " Opt. Express 14, 7515-7534 (2006)

[3] C. Petit, J.-F. Sauvage, T. Fusco (ONERA),J .-L. Beuzit, J. Charton, A. Costille, P. Feautrier, D. Mouillet, P. Puget (IPAG),P. Baudoz, T. Buey, D. Perret, A. Sevin (LESIA), K. Dohlen, J.-L. Gach, E. Hugot (LAM), E. Fedrigo, N. Hubin, M. Kasper, C. Soenke, M. Suarez (ESO), F. Wildi (Geneve Observatory), The SPHERE XAO system SAXO: integration, test and laboratory performance, SPIE (2012).

[4] J.-F. Sauvage, T. Fusco, L. Mugnier, B. Paul, C. Petit, K. Dohlen, "SPHERE non-common path aberrations measurement and pre-compensation with optimized phase diversity processes," SPIE (2011)

[5] Sauvage, J -F; Mugnier, L M; Rousset, G; Fusco, T, Analytical expression of long-exposure adaptive-optics-corrected coronagraphic image. First application to exoplanet detection, JOSAA, Vol. 27, (2010)

[6] Sauvage, J -F; Mugnier, L M; Paul, Baptiste; Villecroze, Rémi; Coronagraphic phase diversity: a simple focal plane sensor for high contrast imaging, Optics Letter, (2012) (submitted)

[7] Paul, B.; Sauvage, J.-F.; Mugnier, L. ; N'Diaye, M. ; Dohlen, K. ; Ferrari, M. ; Fusco, T., Coronagraphic focal-plane wave-front estimation for exoplanet detection: application to the apodized Roddier&Roddier phase mask., SPIE (2012)